

OFDM Carrier Frequency Offset Estimation

Osesina Olukayode Isaac
Yafan Zhang
Pagoti Shirisha

Electrical Engineering Department
Karlstad University
Sweden



June 2006

Internal supervisor: Magnus Mossberg
External supervisor: Lars Lindbom, TietoEnator
Program coordinator: Andreas Jakobsson

Abstract

This thesis discusses and investigates the estimation of carrier offset frequency in orthogonal frequency division multiplexing (OFDM) mobile systems. The investigation starts by using Mobile WiMAX wireless communication specifications described in IEEE 802.16e as the primary system setup. Under this setup orthogonal frequency division multiple access (OFDMA) is used as a physical layer scheme; it also involves the use of pilots in the OFDM symbol for channel estimation.

Although OFDM is resistant to multipath fading, it requires a high degree of synchronisation to maintain sub-carrier orthogonality. Therefore the level of performance of the system depends first on the accuracy in estimating the carrier frequency offset and then the estimation of the channel. Maximum likelihood estimator is used for estimating carrier frequency offset; its performance under different conditions for example SNR, number of virtual carriers needed for estimation etc. are simulated and compared with theoretical results. The optimality of IEEE 802.16e specifications was also examined during the simulations and results analysis.

Acknowledgment

We would like to express our appreciation to our supervisors Dr. Magnus Mossberg, Karlstad University and Dr. Lars Lindbom, TietoEnator and our course co-ordinator Professor Andreas Jakobsson, Karlstad University for their guidance and invaluable time spent during the numerous meetings and consultations we had. Without them then completion of this thesis project would have been impossible.

We would also like to thank our families who supported us morally and financially during our years of education.

CONTENTS

LIST OF FIGURES	iii
LIST OF TABLES	iv
1 INTRODUCTION	1
1.1 Objective	1
1.2 Outline	2
2 OFDM BASICS	3
2.1 Transmitter	5
2.1.1 Forward Error Correction (FEC)	5
2.1.2 Quadrature Amplitude Modulation (QAM) and Symbol Mapping	5
2.1.3 Sub-carrier Allocation	5
2.1.4 IFFT	7
2.2 Receiver	8
2.3 WiMAX	8
2.3.1 IEEE 802.16e	9
2.3.2 Scalable OFDMA	9
3 TRANSMISSION CHANNEL	11
3.1 Channel Model	11
3.1.1 Time-variant and time-invariant channels	11
3.1.2 Dispersive Channel	12
3.1.3 Rayleigh Fading Channels	15
3.1.4 Doppler Effect	16
3.1.5 Delay Spread	17

3.2	Intercarrier Interference (ICI)	18
3.2.1	Intersymbol Interference (ISI)	18
3.3	Cyclic Prefix (CP)	18
3.4	Guard sub-carriers	19
4	FREQUENCY OFFSET AND CHANNEL ESTIMATION	20
4.1	Channel Estimation	20
4.2	Frequency Offset	22
4.3	Maximum Likelihood (ML) Estimation	23
5	SIMULATIONS	31
5.1	Noise Level Tolerance of Phi Estimation	31
5.2	Selection of Number of Virtual Carriers for Estimation	32
5.3	Effect of Noise Level on Channel Estimation	36
6	CONCLUSIONS	40
6.1	Future Work	41
	BIBLIOGRAPHY	42

List of Figures

2.1	Comparison of Bandwidth utilization in FDMA and OFDM.	3
2.2	Basic Architecture of OFDM Systems.	4
2.3	UpLink Tile Structure - IEEE 802.16e.	6
2.4	OFMDA Sub-Carrier Structure.	7
3.1	Fading Channel Divided into Flat Fading Sub-channel.	14
3.2	Channel Delay-Spread (power).	17
3.3	Insertion of Cyclic Prefix (CP).	19
4.1	Channel Estimation Procedure.	21
4.2	$S(\phi, \tilde{d}_{ML})$ structure for 1024 N_{FFT} - $\phi_{true} = 0.4$.	27
4.3	$S(\phi, \tilde{d}_{ML})$ structure for 2048 N_{FFT} - $\phi_{true} = 0.4$.	28
4.4	$S(\phi, \tilde{d}_{ML})$ structure for 3072 N_{FFT} - $\phi_{true} = 0.3$.	28
4.5	$S(\phi, \tilde{d}_{ML})$ structure between 0.01 and 0.05 for 1024 N_{FFT} - $\phi_{true} = 0.3$.	29
5.1	SNR effect on the estimation of ϕ .	32
5.2	Estimation performance with respect to number of used virtual sub-carriers.	33
5.3	SNR effect on ϕ estimation: Comparison between $\hat{\phi}_{i=91}$ and $\hat{\phi}_{i=50}$.	34
5.4	Relative Error of ϕ estimation at different SNR: Comparison between $\hat{\phi}_{i=91}$ and $\hat{\phi}_{i=50}$.	35
5.5	Channel Estimate SNR = 10 dB.	37
5.6	Channel Estimate SNR = 15 dB.	37
5.7	Channel Estimate SNR = 20 dB.	38
5.8	Channel Estimate SNR = 25 dB.	38

List of Tables

2.1	OFDMA Scalability Parameters.	10
3.1	Default mobile speeds for the TUx channel model.	13
3.2	Typical Urban Channel Model (TUx).	13

Chapter 1

INTRODUCTION

Today's mobile communications aims at providing voice and low data rate services, such as GSM, IS-136, and JDC etc. However they cannot efficiently meet the growing demand for mobile services such as multimedia broadband services. Because multimedia communication has a rather large demand on bandwidth and quality of service (QoS) compared to what is available today, alternate ways to transmit large bit stream through the channel with sufficient QoS guarantees are sought.

Orthogonal Frequency Division Multiplexing (OFDM) is an efficient modulation scheme proposed as a solution to this problem. OFDM is a multiple carrier modulation technique. It distributes data over a large number of sub-carriers spaced apart at precise frequencies, such that they are orthogonal to one another.

OFDM has been successfully applied to a wide variety of digital communication applications over the past several years including digital TV broadcasting, digital audio broadcasting, Asynchronous Digital Subscriber Line (ADSL) modems and wireless networking worldwide. Its application in mobile communication is more complex especially because of the mobility of the mobile user; thus more exact symbol timing and frequency-offset control must be used to ensure that sub-carriers remain orthogonal.

However, the difference between the frequency of the oscillator in the transmitter and the receiver causes frequency offset which if not estimated and compensated for could ruin the orthogonality of the sub-carriers thereby causing large bit errors in the received signal. Also the distortion of the signals while traveling through the channel and the movement of the mobility user causes synchronisation problems.

1.1 Objective

The main objective of this thesis is to investigate effective frequency-offset and channel estimation methods in OFDM mobile communications systems. *MATLAB®*

would be the key tool used for the estimation process. A key investigated part would be how pilots can be included in the Maximum Likelihood Estimation (MLE) method in order to reduce the operational cost [1].

Various system settings would be simulated and the results would be compared and analysed. Suggestions about changes that could be made in OFDM symbol structure to increase efficiency for the tested estimation methods would also mentioned.

1.2 Outline

Chapter 1 of this thesis project contains the general introduction to the thesis work, objectives as well as the outline.

Chapter 2 contains the background of OFDM; it includes the differences between single carrier (FDM) and multi-carrier (OFDM) modulation schemes. A basic OFDM architecture figure and description of its various blocks including OFDM symbol construction and symbol mapping are also presented. Quadrature Amplitude Modulation (QAM) is introduced as an appropriate modulation technique for the OFDM sub-carriers. OFDMA parameters with regards to the WiMax configurations used in this thesis are also discussed.

Chapter 3, is focused on the transmission channel. The properties of time-variant and time-invariant channels and its effects on the transmitted signal are described. The channel model equation and assumptions about its properties are also depicted.

Chapter 4 is focused on channel estimation. Estimation of the carrier-frequency offset as well as the channel is treated in details in this chapter. Various estimation techniques are explained in conjunction with their relative merits on SNR performance, overhead and buffering delay.

In Chapter 5, we described the setup and assumptions used in our simulations. Simulation aims, results (plots) and analysis are also detailed in this chapter.

Chapter 6 contains the conclusion of the thesis project and proposals for possible future works.

Chapter 2

OFDM BASICS

In wireless communications, the channel's power spectrum is not consistent in the entire channel frequency band; OFDM divides such a channel into many pieces by frequency called sub-channels; each of the sub-channels consist of sub-carriers. The sub-carrier spacing is carefully selected so that each carrier is located on all the other carrier's spectra zero crossing points, and each sub-channel's power spectrum is relatively consistent. This is explained in Figure 2.1. OFDM utilises the transmission channel efficiently, for example much better than FDMA, Frequency Division Multiplexing Access which is predecessor [7].

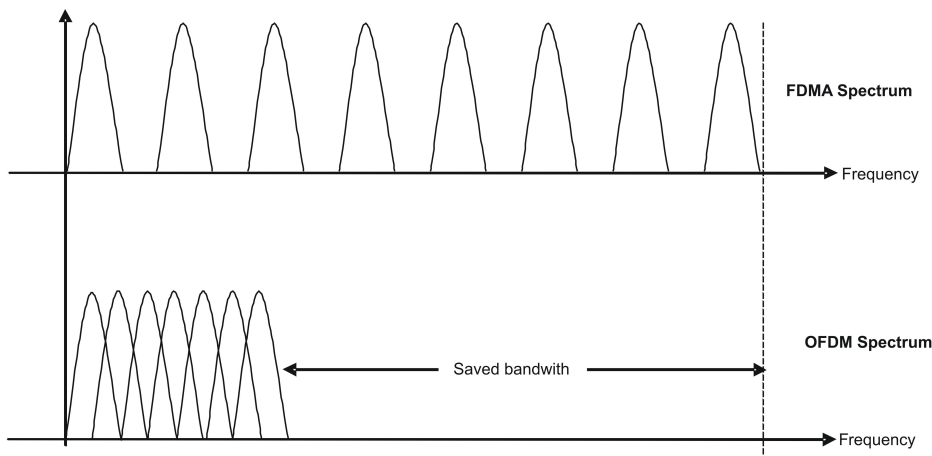


Figure 2.1. Comparison of Bandwidth utilization in FDMA and OFDM.

The main advantage of OFDM is that the sub-carriers can be considered almost flat fading; this enables it to overcome multipath fading in the mobile communication environment. It has high spectral efficiency, resiliency to RF interference and lower multipath distortion; all of which leads to simplified processing at the receiver.

Another advantage of OFDM in mobile communications is that it can be the basis to introduce some adaptive transmission technology such as multimode modulation based on the sub-carriers SNR which can maximize the channel throughput. This is a very useful characteristics, because it can be used to improve the system's spectrum efficiency.

However, OFDM is subject to the system's linearity and synchronization. It needs more exact symbol timing and frequency-offset controlling to ensure that the sub-carriers are orthogonal. Otherwise, the interference of different sub-carriers will lead to a high bit error probability. In mobile communication, schemes that deliver exact synchronisation are hard to implement, especially in high data rate at high moving speed [2].

In OFDM systems, multiple signals are sent out at the same time but on different frequencies. When multiple versions of the signal interfere with each other (inter symbol interference (ISI)), it becomes very hard to extract the original information.

Basic Architecture of OFDM Systems

OFDM system block architecture can be divided into 3 main sections, see Figure 2.2, namely the transmitter, the channel and the receiver. The model used in this thesis is tested without the using the Forward Error Correction (FEC) coding (denoted in double-line box).

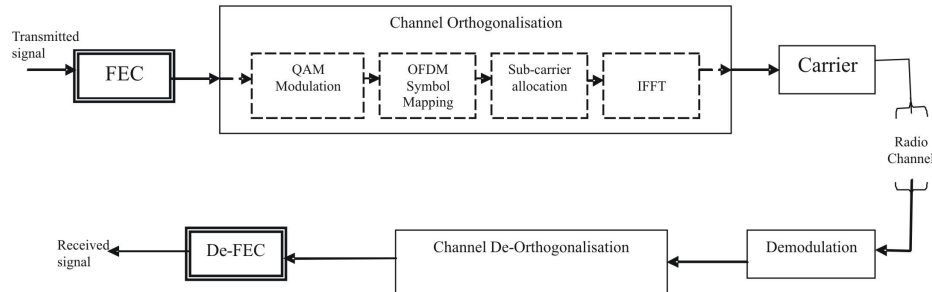


Figure 2.2. Basic Architecture of OFDM Systems.

2.1 Transmitter

2.1.1 Forward Error Correction (FEC)

FEC coding is a technique that improves digital channel quality through the addition of redundant data (parity bits) at the sending node. The redundant data is then decoded at the receiver to detect and correct errors. It is used in OFDM systems to reduce error probability; it trades off data rate and error probability.

There are several coding schemes including Convolution Codes (CC), Binary Turbo Codes (TC) and Turbo Trellis Coded Modulation (TTCM) for an OFDM modulated transmission. In our thesis, FEC is not considered in detail.

2.1.2 Quadrature Amplitude Modulation (QAM) and Symbol Mapping

Many transmitted signals are analog or time continuous in nature, such signals can be converted to their digital or discrete form in order to improve the noise resistance¹. Consequently many transmission systems make of use digital modulation techniques. QAM is one of such techniques; it utilizes the mathematical property that input signals are divided and carried on different components of a single frequency carrier wave, and at the receiver they are resolved successfully into inputs. It is also desirable for high data rate performance [9].

The different QAM modulation schemes commonly used are, e.g., 4-QAM (QPSK), 8-QAM, 16-QAM, 32-QAM and 64-QAM with gray coding in the constellation map. QPSK would be used for simulation purposes in this thesis project, unless otherwise stated. The coded bits (uncoded, if FEC is not used) are then mapped to the constellation map to form the data symbols.

2.1.3 Sub-carrier Allocation

The data symbols are then mapped into OFDM symbols, i.e., they are assigned to (modulated by) different sub-carriers on an OFDM symbol such that they are evenly spaced. Hence the frequency of each sub channel is determined by

$$f_k = \frac{k}{NT_{symbol}} \quad (2.1.1)$$

¹If the noise is purely random over the operating range of a particular signal, oversampling can be used to reduce such random noise. The noise reduction with N samples is $1/\sqrt{N}$ of the original noise level

where k is the sub-carrier index, T_{symbol} is the OFDM symbol period and N is the number of sub-carriers.

Symbols are allocated indices representing the sub-carriers and OFDM time symbol. A sub-channel is a combination of sub-carriers, and a slot (3 OFDM symbols in OFDMA Uplink). Each sub-channel consists of tiles; a tile is the smallest data unit, see Figure 2.3. The tile structure differs in Downlink (DL) and Uplink (UL).

An OFDM frame consists of the DL and UL parts, both totaling 48 OFDM symbols. The DL part of the frame is used to transmit signal from the Base Station (BS) to all assigned Subscriber Stations (SS) using a carrier frequency in broadcast Time Division Multiplex (TDM) with the OFDM method. The UL part is used to transmit signal from the SS sharing the same radio frequency carrier with other assigned SS to the BS in Time Division Multiple Access (TDMA) mode [12].

The guard sub-carriers are used to avoid ISI, to be discussed later. During simulation in this thesis they are given null values, hence the power of the guard sub-carrier is not considered.

The pilot symbols contain information known both by the transmitter and the receiver; they are used for synchronisation and channel estimation.

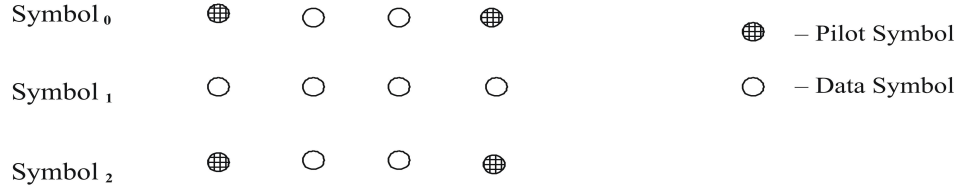


Figure 2.3. UpLink Tile Structure - IEEE 802.16e.

Importance of Orthogonality

The carriers in normal FDM systems can be distinguished (for demodulation) because they are spaced with guard bands (in the frequency domain), see Figure 2.4. In OFDM systems where the sidebands of individual carriers overlap, the carriers must be mathematically orthogonal if they are to be received without adjacent carrier interference. The receiver acting as a bank of demodulators translates each carrier to DC and then integrates the resulting signal over a symbol period to recover the original data. This demand on the receiver is clearly higher than that of

normal FDM where conventional filters and demodulators are used [10].

If the frequencies of other carriers in the time domain occupy a whole number cycles in the symbol period (T_{symbol}), then the integration process results in zero contribution from all these carriers. Hence the carriers are linearly independent (orthogonal) if the carrier spacing is a multiple of $1/(T_{symbol})$.

Suppose we have a set of signals ϕ , where ϕ_l and ϕ_m are the l -th and m -th elements respectively in the set. The signals are orthogonal if

$$\int_a^b \phi_l(t)\phi_m^*(t)dt = \begin{cases} K & \text{for } l = m \\ 0 & \text{for } l \neq m \end{cases} \quad (2.1.2)$$

where ϕ_l and ϕ_m are the sub-carriers l and sub-carrier m respectively.

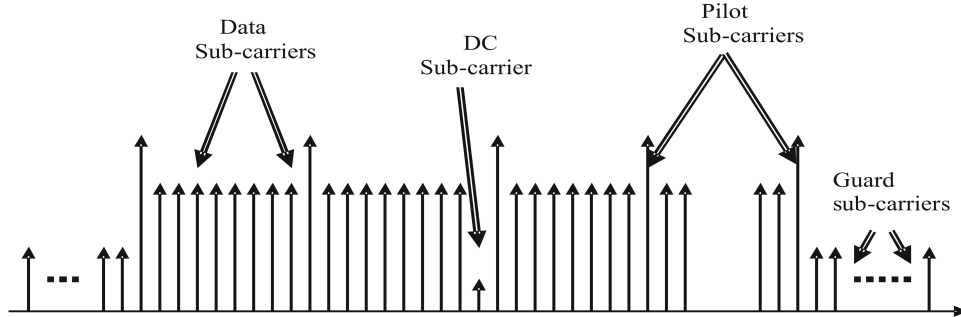


Figure 2.4. OFMDA Sub-Carrier Structure.

2.1.4 IFFT

After the OFDM symbols are stacked up into the frame, it is then converted to time domain using the Inverse Discrete Fourier Transform (IDFT). An efficient way of implementing IDFT is IFFT (Inverse Fast Fourier Transform). IFFT is useful for OFDM because it generates samples of a waveform with frequency components satisfying orthogonality conditions, i.e., the IFFT modulates each sub-channel onto a precise orthogonal carrier [1].

The IDFT of sub-carrier $X(k)$ is given as below; this in effect is equivalent to OFDM symbol generation.

$$x(n) = \frac{1}{N} \sum_{k=0}^{N-1} X(k) e^{j \frac{2\pi k n}{N}}, \quad \text{for } n = 0, \dots, N-1 \quad (2.1.3)$$

2.2 Receiver

The receiver part of the OFDM system will not be discussed in details in this thesis. This thesis would focus on the estimation of the carrier frequency offset before the signal is processed through all the different blocks at the receiver side.

A typical OFDM receiver first removes the cyclic prefix (added to prevent ISI). The data is passed through the serial to parallel converter and then fed to the Fourier Frequency Transform (FFT) for frequency domain transformation. In order to reconstruct the original data from the received data (distorted by the channel), channel estimation and interpolation operations are performed. For this purpose the pilot sub-carriers are used. In this thesis several estimation methods would be mentioned but the Maximum Likelihood (ML) estimation of OFDM carrier frequency offset would be explored [1].

In the presence of time dispersive channel, additive noise and carrier frequency offset, the OFDM signal at the receiver is

$$y(n) = \frac{1}{\sqrt{N}} \sum_{k=0}^{M-1} H(k) d_k e^{j((2\pi k/N) + \Delta\omega \cdot T_s)n} + z(n) \quad (2.2.1)$$

where $H(k)$ is the channel frequency response corresponding to sub-carrier k , $z(n)$ is additive complex Gaussian noise, $M \leq N$ and $N-M$ represents the number of null sub-carriers (or the virtual sub-carriers).

T_s is the symbol interval/sampling time and $\Delta\omega$ is the frequency offset. The normalized phase shift, ϕ is defined as $\phi = \Delta\omega \cdot T_s$

2.3 WiMAX

Worldwide Interoperability for Microwave Access (WiMAX) [4] is a body that ensures that the broadband wireless radios manufactured for customer use interoperate

from vendor to vendor. It provides specifications for both fixed Line-of-sight (LOS) communication in the range of 10-66 GHz, Non-LOS communication in the range of 2-11 GHz. The WiMAX standard to enable the adoption of advanced radio features in a uniform fashion and reduce the radio production costs for companies who are part of the WiMAX Forum - a standards body formed to ensure interoperability via testing.

2.3.1 IEEE 802.16e

Under IEEE 802.16e [2], Mobile WiMAX defines wireless communication specifications for mobiles moving at a speed of 125 km/h in the range of 2-6 GHz. OFDMA is used as the physical layer scheme; the SS uses all the available sub-carriers for the allocated time.

The 802.16 technology would enable the SS to get broadband wireless access (BWA) at all times in all locations, either when stationary, or at pedestrian speed or when traveling at 125 km/h.

2.3.2 Scalable OFDMA

IEEE 802.16e is based on the concept of scalable OFDMA (S-OFDMA). S-OFDMA supports a wide range of bandwidths to flexibly address the need for various spectrum allocation and usage model requirements.

The OFDM symbol structure used in this dissertation is according to the mobile WiMAX specifications as given in Table 2.1 below. The experiments in this thesis work would be focused mainly on the specifications in Table 2.1 [4].

Parameters	Values
System Channel Bandwidth (MHz)	10
Sampling Frequency (F_p in MHz)	11.2
FFT Size (N_{FFT})	1024
Sub-Carrier Frequency Spacing (kHz)	10.94
Useful Symbol Time ($T_b = 1/f$)	91.4 microseconds
Guard Time ($T_g = T_b/8$)	11.4 microseconds
OFDMA Symbol Duration ($T_{symbol} = T_b + T_g$)	102.9 microseconds
Number of OFDMA Symbols per frame	48
Average Null Sub-carriers per symbol	184
Average Pilot Sub-carriers per symbol	280
Average Data Sub-carriers per symbol	560

Table 2.1. OFDMA Scalability Parameters.

Chapter 3

TRANSMISSION CHANNEL

In Non Line-of-sight (NLOS) wireless communication, reflection of the signal from the surroundings results in a received signal which is a combination of the multipath signals. Because these multipaths have different amplitude and phase, they may add-up either constructively or destructively leading to a complex envelope, i.e., fading.

3.1 Channel Model

In any communication system, the ability to assign the right mathematical model to a channel is crucial; it is desirable that we get a very “good” model of the channel. This model gives us a good knowledge of how the channel behaves (distorts) when the signal passes through; it enables us to increase the performance of the system. Some of the properties and features of the transmission channel are describe below [3].

3.1.1 Time-variant and time-invariant channels

A key feature to be considered when describing a channel is whether it is time-variant or time-invariant. In a time-variant channel the frequency response is constant at all times; hence it is easy to estimate because it requires only a single estimation which will hold all through the transmission. In a time-invariant channel the frequency response is dependent on time; the channel in real life usually exhibits this property.

3.1.2 Dispersive Channel

A dispersive channel is a channel that attenuates distinct frequencies, i.e., it affects the transmitted signal differently at different frequencies. This is referred to as a frequency selective channel. Orthogonality between the sub-carriers is destroyed at the receiver due to channel dispersion.

The general model of a dispersive can be described as:

$$h(t) = \sum_{i=1}^L \alpha_{i(t)} \delta(t - \tau_{i(t)}) \quad (3.1.1)$$

where L is the number of taps of the channel. $\alpha_{i(t)}$ is the path gain of path i and $\tau_{i(t)}$ is the path delay of path i ; at time t). Each path gain $\alpha_{i(t)}$ is a complex random variable with uniformly distributed phase and Rayleigh distributed magnitude, see page 15 for “rayleigh distribution”. In the time-invariant case ‘ t ’ is of no importance since the impulse response is constant at all times. In the time-variant case, the channel will affect the transmitted signal differently at different times.

The channel model used in this thesis work is adapted from the 3rd Generation Partnership Project (3GPP TM) technical report [8]. The channel models in their report were chosen as simplifications, or typical realizations of the COST 259 model [16]. It describes the complex range of conditions found in the real world by distributions of channels rather than an occurrence of different channels. COST 259 explicitly specifies the channel models in three environments namely:

- TUx (typical urban channel model)
- RAx (rural area channel model)
- HTx (hilly terrain channel model)

This thesis work focused mainly on TUx. The default mobile speeds and parameters of the typical urban channel model are mentioned in Table 3.2 and Table 3.3 respectively. The tap delays in this model were determined by generating 20 independent identically distributed values from a uniform distribution in the interval $[0.4\sigma_t, 1]$, where σ_t is the rms delay spread. The relative powers of the taps were calculated and then normalized so that the total power in each channel is equal to one.

Channel model	Mobile speed
TUX	3 km/h
	50 km/h
	120 km/h

Table 3.1. Default mobile speeds for the TUX channel model.

Tap number	Relative time (μ s)	average relative power (dB)	doppler spectrum
1	0	-5.7	Class
2	0.217	-7.6	Class
3	0.512	-10.1	Class
4	0.514	-10.2	Class
5	0.517	-10.2	Class
6	0.674	-11.5	Class
7	0.882	-13.4	Class
8	1.230	-16.3	Class
9	1.287	-16.9	Class
10	1.311	-17.1	Class
11	1.349	-17.4	Class
12	1.533	-19.0	Class
13	1.535	-19.0	Class
14	1.622	-19.8	Class
15	1.818	-21.5	Class
16	1.836	-21.6	Class
17	1.884	-22.1	Class
18	1.943	-22.6	Class
19	2.048	-23.5	Class
20	2.140	-24.3	Class

Table 3.2. Typical Urban Channel Model (TUX).

Applying the Fourier transform then gives the sub-channel in the frequency domain as:

$$H_k = \int_0^{\infty} h(\tau) e^{2\pi k \tau / NT} d\tau \quad (3.1.2)$$

OFDM divides this channel into a number of sub-channels which are almost flat fading. For a slowly fading frequency-selective channel, longer symbol durations (narrow frequency bands) are desirable for mitigating the effect of multipath. However, longer symbol durations are more prone to frequency dispersion due to temporal channel variations. The time-frequency dispersion induced by a time-varying multipath channel destroys the orthogonality condition in the above systems. As a result, there is interference between different basis functions at the receiver.

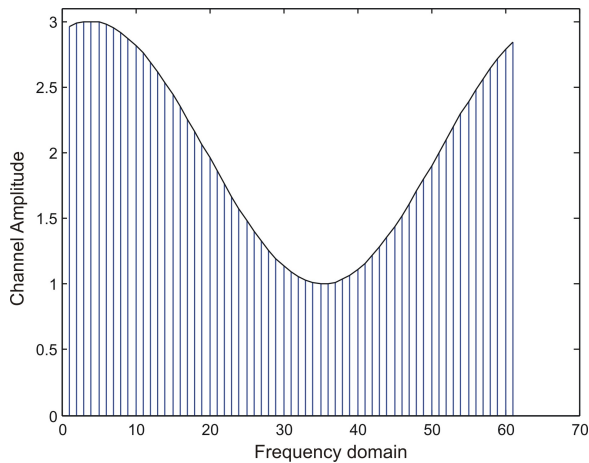


Figure 3.1. Fading Channel Divided into Flat Fading Sub-channel.

With cyclic prefix (CP) and IFFT/FFT processing, the frequency selective fading channel can be easily converted into parallel flat fading sub-channels. In flat fading the same degree of fading takes place for all of the frequency components transmitted through a radio channel and within the channel bandwidth, making the estimation process simpler.

In equation (3.1.1) if the value of M is 1 the channel will constitute of only one tap, then the frequency spectrum is said to be flat. From a frequency domain point of view, the fact that the channel's frequency response is not flat means that the channel output signal differs from the input by more than just a scaling plus noise (the noise is assumed to be Gaussian). In other words the channel filters the transmitted signal and adds noise to it.

A channel is said to be fast fading or slow fading depending on the real difference between two consecutive time instants, e.g., t_0 to t_1 . These terms are also relative to the symbol period; fast fading occurs when the channel changes (not constant) within one symbol period while slow fading occurs when the channel is constant within at least one symbol period.

Fast fading: Coherence time < Symbol period [$T_c < T_{symbol}$]

Slow fading: $T_c > T_{symbol}$

Where T_c is the coherence time (length of time before the channel disperses) and T_{symbol} is the symbol time.

The impact of the environment on the transmitted signal (fading) can also be classified as:

- Long-term fading: it is caused as a result of reflection from the geographical surroundings, e.g., landscape, natural vegetation. Because it varies slowly compared to the symbol time and mostly affect the symbol, it is not of interest when estimating a channel (BW of Signal < BW of channel, Delay spread < symbol period).
- Short-term fading: it is caused by the reflection of the signal from the near environment, e.g., buildings, trees and other small obstacles. It is very interesting when estimating a channel because it varies faster than the symbol time (BW of Signal > BW of channel, Coherence time < symbol period).

3.1.3 Rayleigh Fading Channels

When information is transmitted in an environment with obstacles (Non Line-of-sight - NLOS), more than one transmission paths will appear as result of the reflection(s). The receiver will then have to process a signal which is a superposition of several different transmission paths. If there exists a large number of transmission paths they may be modeled as statistically independent; the central limit theorem will give the channel the statistical characteristics of a Rayleigh Distribution [17].

$$p(\alpha) = \frac{\alpha}{\sigma^2} e^{-\alpha^2/2\sigma^2}, \quad \alpha \geq 0 \quad (3.1.3)$$

where $p(\alpha)$ is the rayleigh distribution, α is the envelope amplitude ¹ of the received signal and $2\sigma^2$ is the predetection mean power ² of the multipath signal.

Small-scale fading refers to the dramatic changes in signal amplitude and phase that can be experienced as a result of small changes (as small as a half-wavelength) in the spatial separation between a receiver and transmitter. It manifests itself in

¹Envelop signal is defined as $g(t) = g_I(t) + jg_Q(t)$, where $g(t)$ is WSS (wide-sense stationary) complex Gaussian random process, amplitude $\alpha(t) = |g(t)|$.

²Predetection Signal Power = average energy per unit time = (energy per symbol)(symbol rate).

two mechanisms, namely, time-spreading of the signal (or signal dispersion) and time-variant behaviour of the channel. For mobile radio applications, the channel is time-variant because the relative change in motion between the transmitter and receiver results in change in the propagation path. The rate of change of these propagation conditions accounts for the fading rapidity (rate of change of the fading impairments).

3.1.4 Doppler Effect

The main factor that affects the rate of fading is the mobility of the receiver relative to transmitter. As the receiver moves with some velocity relative to the transmitter, the phase shifts of the received signal changes. This phenomenon is known as the Doppler shift.

The Doppler rate gives information about how fast the channel is varying compared to the data rate.

In general, doppler frequency, f_d is given by:

$$f_d = f_{d_{max}} \cos \theta \quad (3.1.4)$$

where

θ is the angle of the signal direction

and

$$f_{d_{max}} = \frac{v f_c}{c} \quad (3.1.5)$$

$f_{d_{max}}$ is the maximum Doppler frequency , v is the velocity of the receiver, f_c is the carrier frequency and c is the propagation velocity of the transmitted signal (speed of light).

In mobile radio channels, the maximum Doppler spread is an important parameter used in adaptation (optimize the systems performance, enhance its capacity and utilize available resources in an efficient manner).

3.1.5 Delay Spread

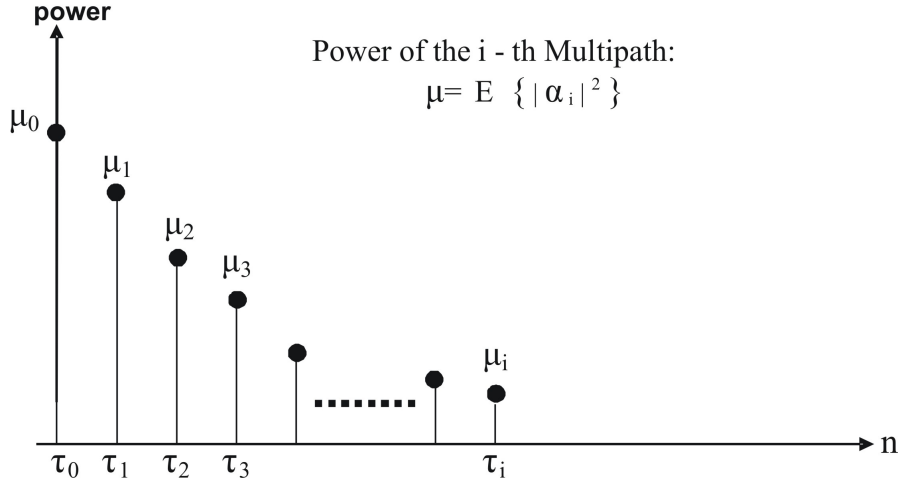


Figure 3.2. Channel Delay-Spread (power).

Note that $\alpha_{i(t)}$ is the gain of each path; $\tau_{i(t)}$ is the path delay of path i .

Multipath Delay-spread RMS value (the square Root of the Mean of the Square of the function),

$$\tau_{rms} = \sqrt{\frac{\sum_i (\tau_i - \tau_m)^2 \mu_i}{\sum_i \mu_i}},$$

where Mean Access Delay, $\tau_m = \frac{\sum_i \tau_i \mu_i}{\sum_i \mu_i}$.

As discussed earlier, slow (short-term) fading is the outcome of the signal reflections on small obstacles in the near surroundings. When modeling the channel, the channel delay spread is closely related to these reflections. Figure 3.2 illustrates the channel delay-spread power at different time instants. The value of τ (in equation (3.1.1)) decides the difference in time between the shortest and the longest transmission path that reaches the receiver.

As delay spread increases, symbol duration should also increase for two reasons:

- First, most receivers require a near-constant channel in each frequency sub-band; as delay spread increases, this can be achieved by an increase of the symbol length.

- Second, to prevent ISI; the length of the guard interval should increase as well. Therefore, to reduce redundancy, the symbol length should increase.

3.2 Intercarrier Interference (ICI)

The effect of channel fading on OFDM symbols is the destruction of the orthogonality of the sub-carriers. The broadening of the signal spectrum of the sub-carriers by the Doppler shift makes them (sub-carriers) to overlap, thereby causing ICI. Due to this phenomenon, OFDM becomes very sensitive to frequency offset. This problem can be solved by introducing CP.

3.2.1 Intersymbol Interference (ISI)

Because the spectra of an OFDM signal is not strictly band limited, linear distortion such as multipath cause each sub-channel to spread energy into the adjacent channels; this causes the previously sent signal to interfere with the currently sent signal. This situation is called ISI. By inserting guard sub-carriers, this problem could be solved.

3.3 Cyclic Prefix (CP)

CP [13] is used in OFDM to combat ISI. The basic idea is to copy part of the OFDM time-domain waveform from the back of the signal to the front to create a guard period, see Figure 3.3. Where the duration of the guard time is chosen such that it is longer than the worst-case delay spread of the targeted multipath environment. CP also makes the channel appear circular and permits low-complexity frequency domain equalization. However, a disadvantage is that it introduces overhead which reduces bandwidth efficiency [4].

The sampling starting point at the receiver is chosen within the CP. This condition ensures that the previous symbol will only have effect over samples within the CP. Another advantage of using CP for the guard symbol is that it helps to maintain the receiver carrier synchronization; some signals instead of a long silence is transmitted [4].

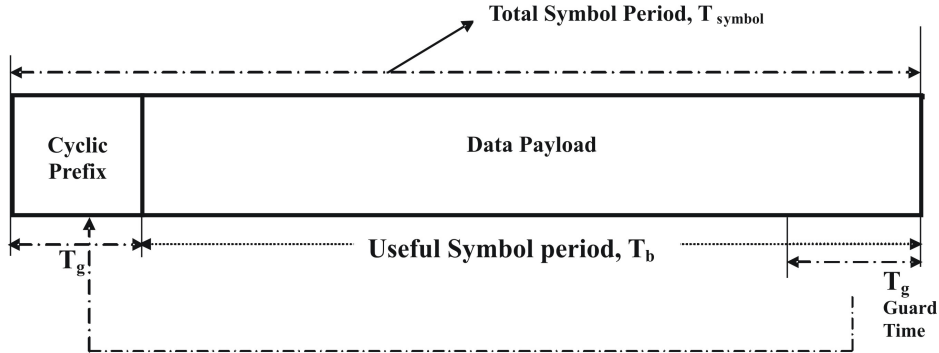


Figure 3.3. Insertion of Cyclic Prefix (CP).

3.4 Guard sub-carriers

By inserting guard sub-carriers we can separate two successive OFDM symbols. Designing the guard interval as a number of null carriers or CP as described above eliminates ISI problem. The guard time specification in IEEE 802.16e is 11.4 microseconds for FFT size of 1024, see Table 2.1.

Chapter 4

FREQUENCY OFFSET AND CHANNEL ESTIMATION

4.1 Channel Estimation

Channel estimation is the process of characterizing or analysing the effect of the physical medium on the input sequence (transmitted data). The basic channel block diagram of channel estimation procedure is shown in Figure 4.1. The primary importance of channel estimation is that it allows the receiver to take into account the effect of channel on the transmitted signal, secondly channel estimation is essential for removing ISI, noise rejection techniques etc. In wideband mobile communications systems, a dynamic estimation of the channel is essential before the demodulation of OFDM signals because the radio channel is time-varying and frequency selective [15].

There are two main types of channel estimation methods, namely blind methods and training sequence methods. In blind methods, mathematical or statistical properties of transmitted data are used. This makes the method extremely computationally intensive and thus hard to implement on real time systems. In training sequence methods or non-blind methods, the transmitted data and training sequences known to the receiver are embedded into the frame and sent through the channel.

Generally, the length of the training sequence is twice or thrice the order of the channel and it is computationally simple compared to blind methods. One of the popular methods is to make use of the training bits (pilot symbols) known to the receiver. The transmitter periodically, inserts the symbol from which the receiver derives its amplitude and phase reference. Although training sequence method is much less computationally intensive than the blind methods, the channel bandwidth is not put into effective use by the transmission of training sequences.

Another channel estimation method is called semi-blind method. The semi-blind methods use information from both training sequence and statistical properties of the transmitted signal, which makes them more robust than the blind methods

while they still require less training compared to the non-blind methods.

It is preferable to estimate the channel before converting the received signal to time domain so as to reduce or eliminate the risk of compounded error. Therefore in this project, frequency domain channel estimator is designed and simulated.

In OFDM system, data are modulated on frequency domain sub-channels and scaled by different sub-channel frequency response coefficients after passing through the multipath channel. For coherent detection, these sub-channel frequency responses must be estimated. This estimation is usually done using training symbols which are embedded in the symbol. In this thesis pilots are used for channel estimation. A possible way of performing channel estimation is illustrated in Figure 4.1.

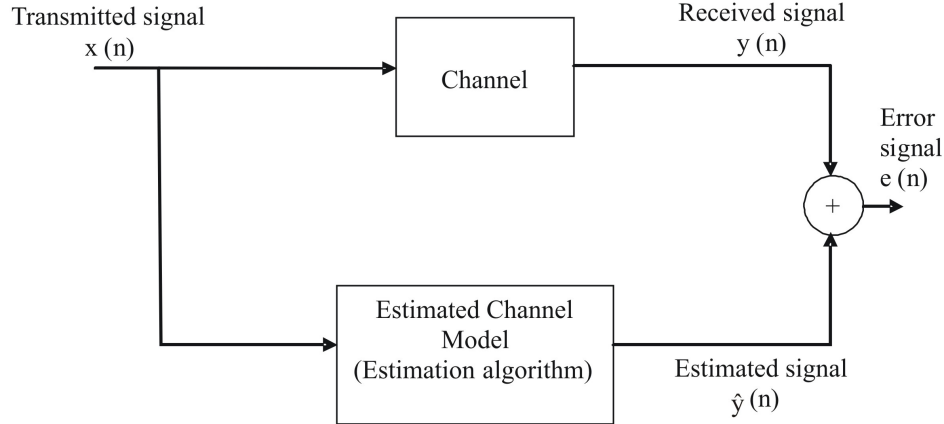


Figure 4.1. Channel Estimation Procedure.

In an OFDM receiver, channel estimation is performed in frequency-domain on the signal output from the FFT block. The received signal after passing through the channel can be described as [14].

$$y(n) = H(k)x(n) + z(n) \quad (4.1.1)$$

where k is the sub-channel (or sub-carrier) index, $y(n)$ is the signal output from the FFT, $H(k)$ is the channel frequency response corresponding to sub-carrier k , and $z(n)$ is the noise. If the FFT input noise is white, the output noise is also white.

4.2 Frequency Offset

The sensitivity of OFDM systems to frequency offset compared with single carrier systems is a major disadvantage. In general, Frequency offset is defined as the difference between the nominal frequency and actual output frequency.

In OFDM, the uncertainty in carrier frequency, which is due to a difference in the frequencies of the local oscillators in the transmitter and receiver, gives rise to a shift in the frequency domain. This shift is also referred to as frequency offset. It can also be caused due to the Doppler shift in the channel. The demodulation of a signal with an offset in the carrier frequency can cause large bit error rate and may degrade the performance of a symbol synchronizer. It is therefore important to estimate the frequency offset and minimize/eliminate its impact [11].

If frequency offset is denoted as Δf_c , the OFDM signal generated by the transmitter denoted as $s(t)$ and $y(t)$ is the signal received by the receiver, then

$$s(t) = e^{j\omega t} x(t) \quad (4.2.1)$$

$$y(t) = e^{j(\omega - \hat{\omega})t} x(t) \quad (4.2.2)$$

$$\Delta\omega = \omega - \hat{\omega} = 2\pi\Delta f_c \quad (4.2.3)$$

Then the received signal has phase offset equal to

$$y(nT) = e^{j\Delta\omega nT} x(nT) \quad (4.2.4)$$

$$\phi(n) = \Delta\omega nT \quad (4.2.5)$$

The frequency response of each sub-channel should be zero at all other sub-carrier frequencies, i.e., the sub-channels shouldn't interfere with each other. The effect of frequency offset is a translation of these frequency responses resulting in loss of

orthogonality between the sub-carriers and leading to ICI.

There are several channel estimation algorithms, for example first and second orders linear Interpolation, Linear Minimum Square Error (LMSE) and Maximum Likelihood (ML) - (least square in time domain). In this thesis, ML estimator method is presented to estimate both the carrier frequency offset (CFO) and the channel of each user in OFDMA systems.

4.3 Maximum Likelihood (ML) Estimation

ML is known to provide a consistent approach to parameter estimation problems and becomes minimum variance unbiased with the increase in the sample size. Assuming that the noise in the channel $z(n)$ is Gaussian, it would be hard to get a better estimate than that of ML estimate. Hence, ML estimate is chosen as a benchmark with which we analyse our thesis work. However, ML estimates can be sensitive to starting values and can also be heavily biased for small samples [18].

During ML estimation procedure of frequency offset in OFDM, we assume that only the first M sub-carriers out of N sub-carriers in an OFDM symbol are used as information sub-carriers, equivalently the information symbols corresponding to the last $N-M$ sub-carriers can be assumed to be null. This is the motivation to partition the IDFT matrix as follows [1]:

$$U = \frac{1}{\sqrt{N}} \begin{bmatrix} 1 & 1 & \cdots & 1 \\ 1 & e^{j\omega} & \cdots & e^{j(N-1)\omega} \\ \vdots & \vdots & \ddots & \vdots \\ 1 & e^{j(N-1)\omega} & \cdots & e^{j(N-1)^2\omega} \end{bmatrix} = [W | V] \quad (4.3.1)$$

where N is the size of the FFT, $\omega = 2\pi/N$ corresponds to the carrier spacing in OFDM modulation, W consists of the first M columns of U . V consists of the last $N-M$ columns of U .

U is an orthonormal matrix. Also $W^H V = 0$ and $WW^H + VV^H = I$.

The discrete-time OFDM signal model is

$$s(n) = \frac{1}{\sqrt{N}} \sum_{k=0}^{M-1} d_k e^{j2\pi n k / N} \quad (4.3.2)$$

where n ranges from $n = 0, 1, \dots, N-1$ and each d_k is used to modulate the sub-carrier $e^{j2\pi nk/N}$.

This can be written in matrix form

$$s = Wd \quad (4.3.3)$$

where $d = [d_0, \dots, d_{M-1}]^T$ is the symbol vector.

In the presence of time dispersive channel, additive noise and carrier frequency offset, the OFDM signal at the receiver can be written as

$$x(n) = \frac{1}{\sqrt{N}} \sum_{k=0}^{M-1} H(k) d_k e^{(j2\pi k/N + \Delta w \cdot T_s)n} + z(n) \quad (4.3.4)$$

where $H(k)$ is the channel frequency response corresponding to sub-carrier k , $z(n)$ is additive complex Gaussian noise, T_s is the QAM symbol period, i.e., the sampling frequency and Δw is the frequency offset.

By defining the phase shift, ϕ is defined as $\phi = \Delta w T_s$, then ϕ and Δw differ only by a constant scalar, therefore the estimation of Δw is equivalent to estimation of the normalized phase shift ϕ .

The received signal model written in matrix form is as follows:

$$x = PWd + z \quad (4.3.5)$$

where H is a $M \times M$ diagonal matrix with diagonal element being $H(k)$ and matrix P accounts for the phase shift due to the frequency offset and is defined as $P = \text{diag}(1 e^{j\phi} \dots e^{j(N-1)\phi})$.

If we denote the estimated received symbol as \tilde{d} , then $\tilde{d} = Hd$,

$$x = PW\tilde{d} + z \quad (4.3.6)$$

Assuming that z is complex Gaussian with covariance matrix $\sigma^2 I$, the likelihood

function of ϕ and \tilde{d} is [1]

$$L(\phi, \tilde{d}) = \frac{1}{(\pi\sigma^2)^N} \cdot \exp \left\{ -\frac{1}{\sigma^2} (x - PW\tilde{d})^H (x - PW\tilde{d}) \right\} \quad (4.3.7)$$

Thus the Maximum likelihood estimate for ϕ and \tilde{d} is given by

$$(\phi_{ML}, \tilde{d}_{ML}) = \arg \max_{\phi, \tilde{d}} \ln L(\phi, \tilde{d}) \quad (4.3.8)$$

simultaneously if $S(\phi, \tilde{d})$ is minimized, we get

$$S(\phi, \tilde{d}) = (x - PW\tilde{d})^H (x - PW\tilde{d}) \quad (4.3.9)$$

Then the gradient of $S(\phi, \tilde{d})$ with respect to ϕ and making to zero gives rise to

$$W^H P^H (x - PW\tilde{d}) = 0 \quad (4.3.10)$$

By solving the above equation, we get \tilde{d}_{ML}

$$\tilde{d}_{ML} = W^H P^H x \quad (4.3.11)$$

By substituting this value of \tilde{d}_{ML} in $S(\phi, \tilde{d})$, we get

$$\begin{aligned} S(\phi, \tilde{d}_{ML}) &= (x - PWW^H P^H x)^H (x - PWW^H P^H x) \\ &= x^H (I - PWW^H P^H)^H (I - PWW^H P^H) x \\ &= x^H (I - PWW^H P^H) x \end{aligned} \quad (4.3.12)$$

By performing joint minimization with respect to (ϕ, \tilde{d}_{ML}) which replaces with

a two step minimization, the ML estimate for d is of the same form as in the above equation(4.3.11) for all possible values of ϕ is to be noticed. By considering further that $PP^H = P^H P = I$, we get

$$\begin{aligned}
 S(\phi, \tilde{d}_{ML}) &= x^H PP^H(I - PW P^H)PP^H x \\
 &= (P^H x)^H(I - WW^H)P^H x \\
 &= (P^H x)^H VV^H P^H x \\
 &= (P^H x)^H \left(\sum_{i=M}^{N-1} u_k u_k^H \right) P^H x \\
 &= \sum_{i=M}^{N-1} \|x^H P u_k\|^2
 \end{aligned} \tag{4.3.13}$$

Here V is same as defined in equation (4.3.1), where u_k are columns with $i = M, \dots, N-1$. So, V has all the last $N-M$ columns of U matrix.

Estimation steps:

1. Estimate ϕ by minimising equation(4.3.13). This is done by trying various values of ϕ ; $\phi = \phi_1, \phi_2, \dots, \phi_{max}$
where $\phi_{max} = T_b \Delta\omega_{max}/N_{FFT}$ and $T_s = T_b/N_{FFT}$
 $\Rightarrow \phi_{max} = T_s \Delta\omega_{max}$

The ϕ that minimizes the equation above is then selected, ϕ_{ML} . $\Delta\omega_{max}$ is the allowed maximum frequency offset, usually specified by the standard of the mobile radio system.

2. Solve for the ML estimated received data (without the knowledge of the channel) using: $\tilde{d}_{ML} = W^H P x$, where $P = \text{diag}(1 e^{j\phi_{ML}} \dots e^{j(N-1)\phi_{ML}})$.
3. Estimate H_{pilot} by using $\tilde{d}_{ML,pilot} = \hat{H} d_{pilot}$.
4. Interpolate \hat{H}_{pilot} values to get \hat{H}_{data} .
5. d_{data} is then obtain from $d_{ML,data} = \hat{H}_{data} d_{data}$.

In case the search included several local minima, first we set the search resolution and search for the first minimum, ϕ_1 (between 0 and ω). The search is then continued starting from ϕ_1 with an interval of ω between every ϕ until the end of the concerned region. Step 2 through 5 as described above is then followed.

Note: The first search is carried out between 0 and ω and the second search is done with an interval of ω between every ϕ because the period of the minima is ω .

Investigating the structure of the cost function in equation 4.3.13 by plotting the values of the cost function for different values of phi with intervals of 0.01 between the range 0 and 0.8, see Figures 4.2, 4.3 and 4.4. They show that it does not monotonically converge to the global minimum, however there is a clear periodicity of the occurrence of the local minima.

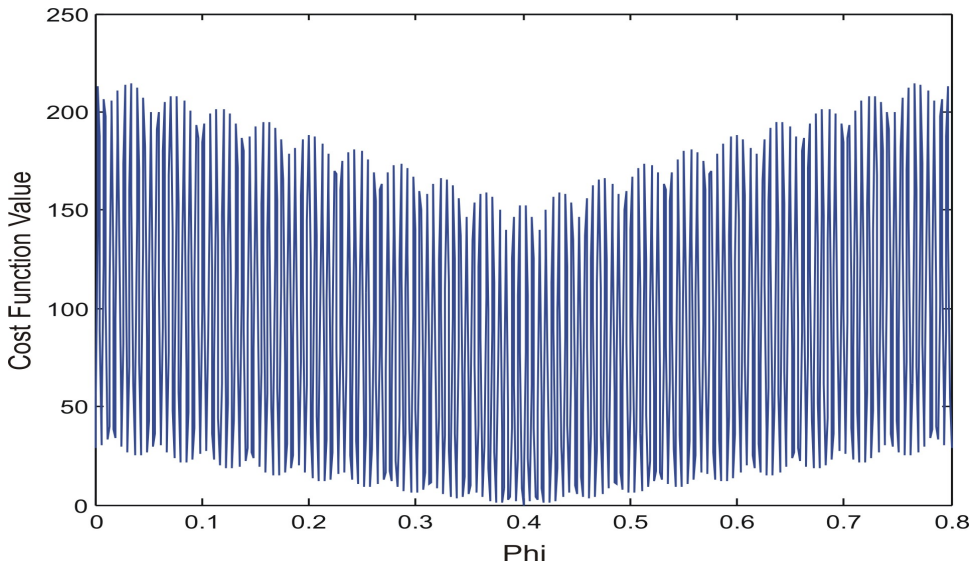


Figure 4.2. $S(\phi, \tilde{d}_{ML})$ structure for 1024 N_{FFT} - $\phi_{true} = 0.4$.

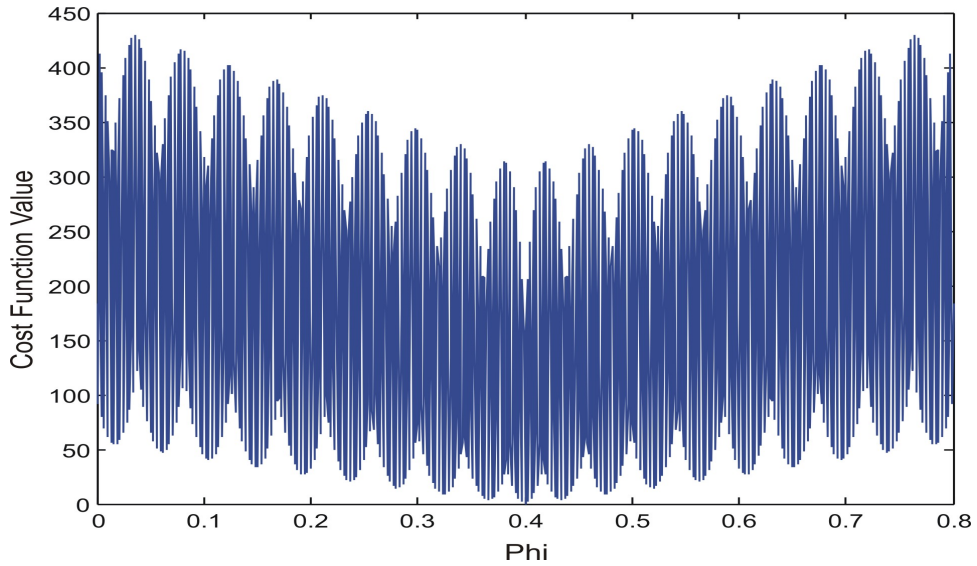


Figure 4.3. $S(\phi, \tilde{d}_{ML})$ structure for 2048 N_{FFT} - $\phi_{true} = 0.4$.

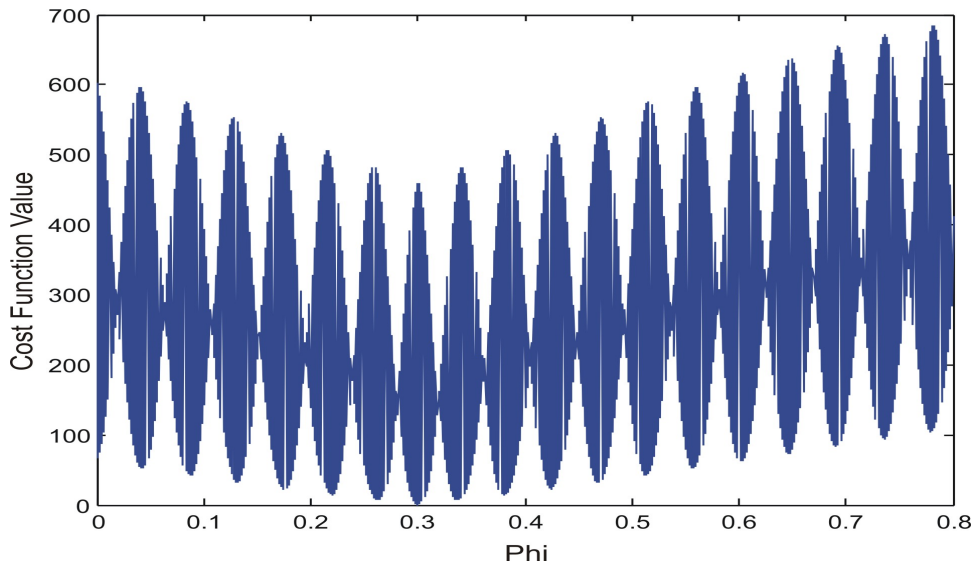


Figure 4.4. $S(\phi, \tilde{d}_{ML})$ structure for 3072 N_{FFT} - $\phi_{true} = 0.3$.

Further, closer investigation of the cost function revealed more local minima, see Figure 4.5 than the ones in the above figures. The occurrence of these many local minima makes the search for the minimising phi very costly if the search range is wide. This can be illustrated by plotting the values of the cost function for several phi values between 0.01 and 0.05 when the true phi is 0.03.

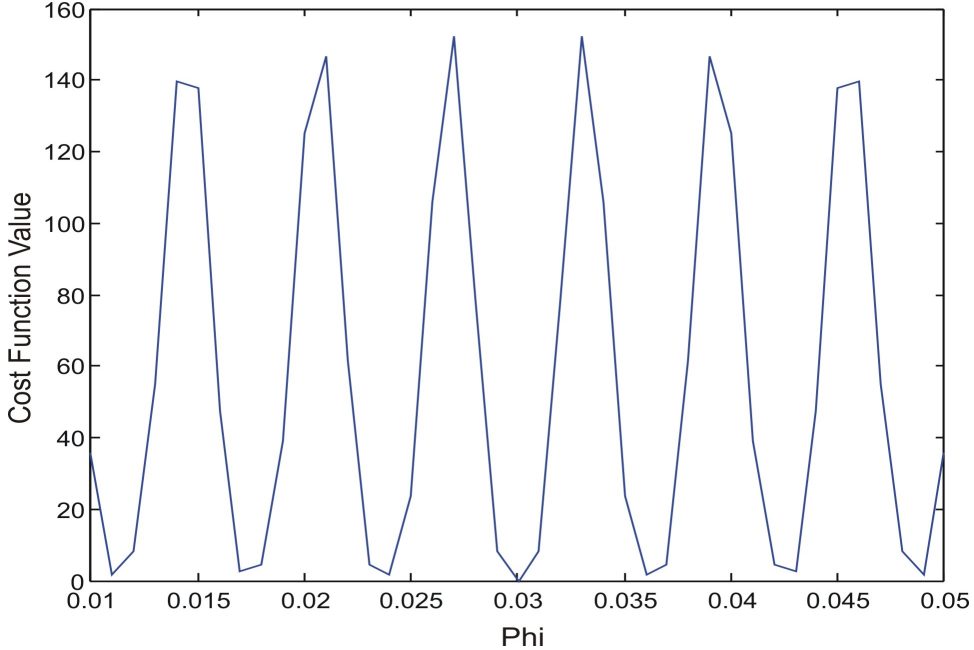


Figure 4.5. $S(\phi, \tilde{d}_{ML})$ structure between 0.01 and 0.05 for 1024 N_{FFT} - $\phi_{true} = 0.3$.

By using the property of the structure, i.e, the periodicity of the (first) local minima, $\omega = 2\pi/N_{FFT}$ and the specification of the maximum frequency offset allowed in 802.16e, $\omega_{max} = 2\%$ of the sub-carrier spacing, the estimation becomes much more cheaper. From Table 2.1, the sub-carrier frequency spacing is 10.94 kHz. Hence $\Delta\omega_{max} = 218.8\text{Hz}$.

$$\begin{aligned}
 \phi_{max} &= \frac{T_b \Delta\omega_{max}}{N_{FFT}} \\
 &= \frac{91.4\mu\text{s} \cdot 218.8\text{Hz}}{1024} \\
 &= 1.953 \times 10^{-5} < 0.0061 = \omega (= 2\pi/1024)
 \end{aligned}$$

Because ϕ_{max} is less than ω (for cases when T_b and $\Delta\omega_{max}$ are in the range above), it is enough to carry out the search between 0 and ω .

Chapter 5

SIMULATIONS

WiMAX specifications used in the setup of the simulations are the following:
FFT size = 1024, First 92 and last 91 sub-carriers are used as guards and Uplink tile structure.

5.1 Noise Level Tolerance of Phi Estimation

As the signal-to-noise (SNR) ratio increases, the accuracy with which phi is estimated can also be expected to increase. In the next simulation exercise, we aim to find the least SNR for which the accuracy of our estimation result is acceptable. Using an ideal channel ($H = 1$), the mean square error (MSE) of phi was plotted for SNR values between 5 dB and 30 dB (with an interval of 5 dB) in figure 5.1. This was repeated for 200 iterations, at each iteration a new noise signal is used for computation.

$$MSE(\hat{\phi}) = E \left\{ (\hat{\phi} - \phi)^2 \right\}$$

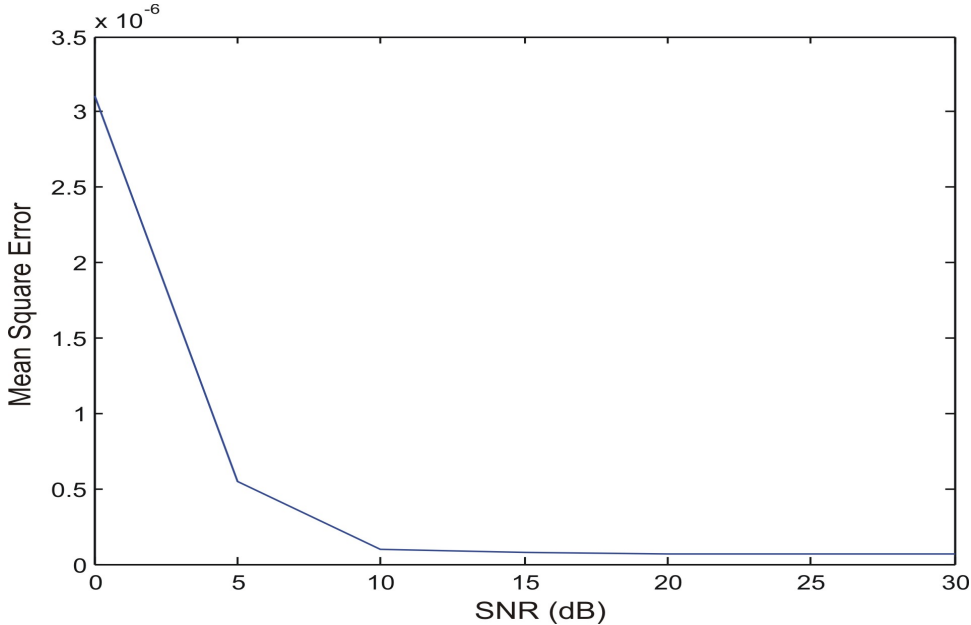


Figure 5.1. SNR effect on the estimation of ϕ .

According to the result plotted above, for SNR level above 10 dB the accuracy of estimation of phi is not greatly affected. However, the estimation scheme's performance is significantly affected for SNR values less than 10 dB.

The MSE does not approach zero for high SNR values ($\text{SNR} \rightarrow \infty$), because the resolution of the estimated ϕ is not fine enough. For high SNR values, the MSE function is more sensitive to the search resolution. Hence, if the resolution of the estimation (ϕ search) is finer (more accurate) enough, the MSE would approach zero as $\text{SNR} \rightarrow \infty$. In the above experiment the same search resolution is used for all the investigated SNR values.

5.2 Selection of Number of Virtual Carriers for Estimation

Theoretically (see equation 4.3.13), the ML estimator requires the use of $i = M, M+1, M+2, \dots, (N_{FFT} - 1)$ virtual carriers for estimation (under 802.16e: 1024 N_{FFT} $i = 934, 935, \dots, 1024$). This is a costly operation and should be reduced if possible. In the next simulation exercise, we investigate if it is possible to perform the estimation with only a part of the i virtual carriers, with an acceptable accuracy. If so, how many virtual carriers is can be used for estimation?

For the simulation setup, we repeated the estimation of ϕ 1000 times using an

ideal channel ($H = 1$). Each time the estimation was done using $i = M, M+1, M+2, \dots, N_{FFT} - 1$; then the MSE averaged over the 1000 iterations was the plotted against the number of elements in i in figure 5.2.

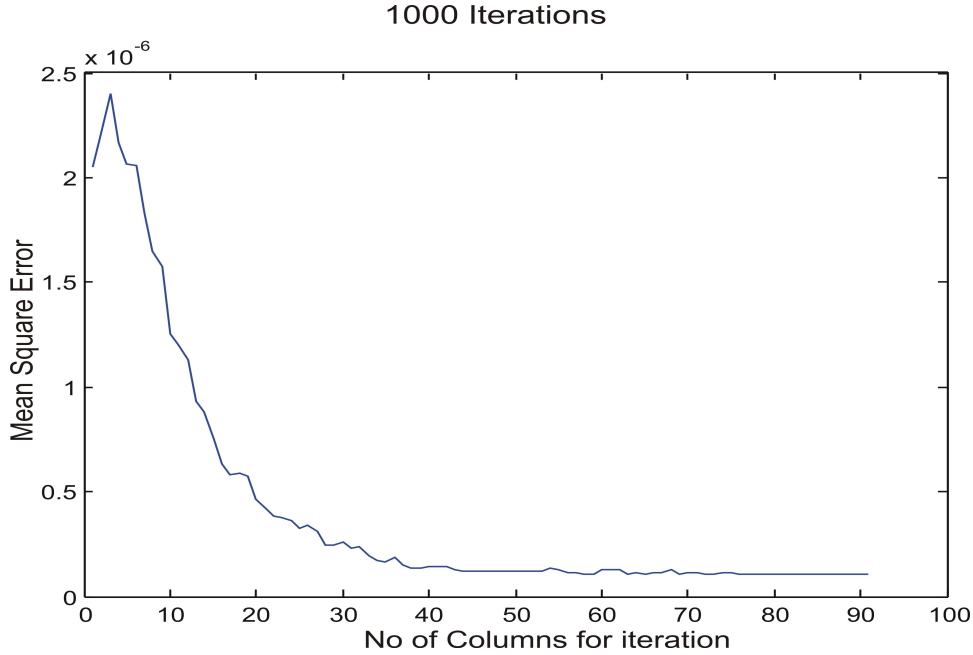


Figure 5.2. Estimation performance with respect to number of used virtual subcarriers.

According to figure 5.2, by choosing $i = 50$, ϕ can be estimated without any significant impact on the estimation accuracy. Hence, the cost of estimation is reduced almost by half.

Now that we have chosen the number of virtual carriers enough for estimation, $i_{enough} = 50$, it would be interesting to see how the estimation of ϕ using i_{enough} is affected by SNR. For this experiment, the simulation step in Section 5.1 was repeated using only i_{enough} number of virtual carriers. The resulting plot is then compared with Figure 5.1.

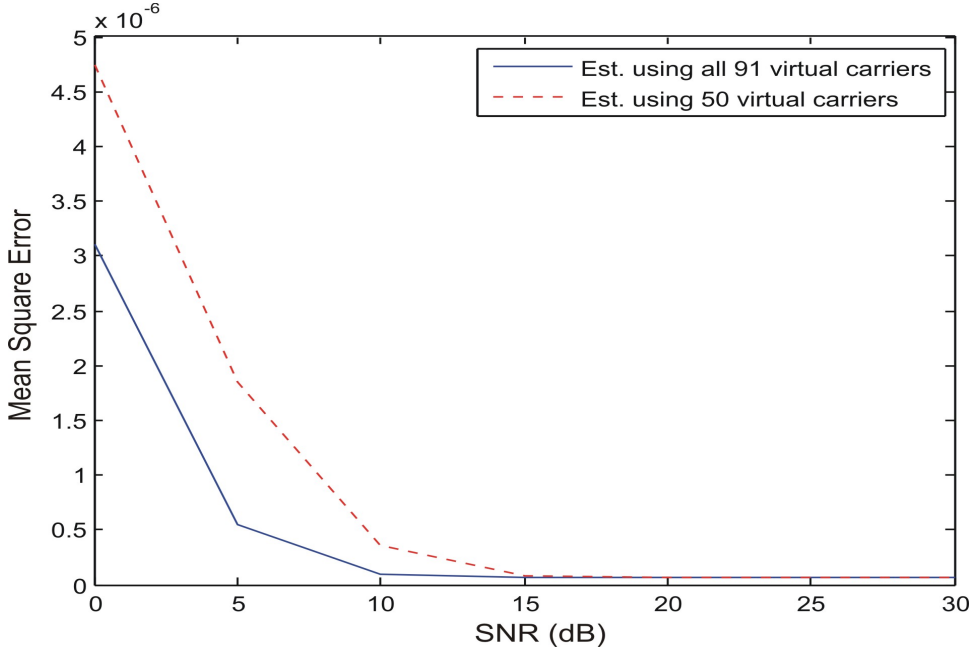


Figure 5.3. SNR effect on ϕ estimation: Comparison between $\hat{\phi}_{i=91}$ and $\hat{\phi}_{i=50}$.

We observed from the above figure that when 91 virtual carriers are used for the estimation of ϕ , the estimation accuracy (MSE) settles (does not change significantly) for SNR values above 10 dB, however when 50 virtual carriers are used, the estimation accuracy settles only for SNR values above 15 dB. Hence, it is desirable to use all 91 virtual carriers when operating the system in an environment where the SNR is less than 15 dB, otherwise using 50 sub-carriers is more desirable.

In order to get a sense of the magnitude of the error $(\hat{\phi} - \phi)$ compared to ϕ itself, we plotted the relative error against SNR.

$$\text{Relative Error} = \frac{\sqrt{MSE}}{\phi} \quad (5.2.1)$$

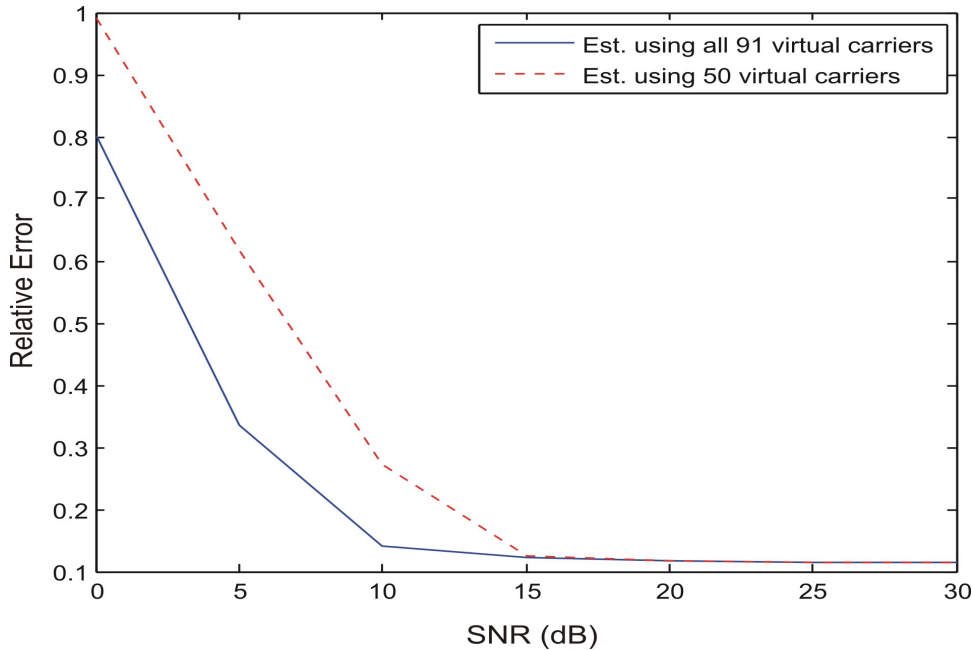


Figure 5.4. Relative Error of ϕ estimation at different SNR: Comparison between $\hat{\phi}_{i=91}$ and $\hat{\phi}_{i=50}$.

The relative error when using 91 virtual carriers settles (steady state) faster than when 50 virtual carriers are used for estimation. In both cases, at steady state the relative error is approximately 10% of ϕ , i.e., we have a 10% accuracy. Depending on particular situations, decision would be made as to the acceptability of this accuracy.

5.3 Effect of Noise Level on Channel Estimation

The aim of our next experiment is to investigate the effect of the level of SNR on channel estimation. We used the TUX channel model described in Table 3.2 to compute $H(k)$.

$$\begin{aligned}
 H(k) &= \sum_{l=1}^L h_l e^{(-j\omega_k \tau_l)} \\
 \omega_k &= \frac{2\pi k}{N_{FFT} T_s} \\
 T_s &= \frac{T_b}{N_{FFT}} \\
 k &= 0, 1, 2, N_{FFT} - 1 \\
 l &= 1, 2, 3, \dots, 20 \\
 h_l &= \text{Average Relative Power (Table 2.3)} \\
 \tau_l &= \text{Relative Time (Table 2.3)}
 \end{aligned} \tag{5.3.1}$$

T_s is the sampling time; T_b is the useful symbol time In our simulation setup:

$$\begin{aligned}
 T_s &= \frac{91.4\mu s}{1024} \approx 0.09\mu s \\
 \omega_k &= \frac{2\pi k}{1024 \cdot 0.09\mu s} \\
 \text{where } k &= 1, 2, 3, \dots, 1024
 \end{aligned}$$

The channel estimate, $\hat{H}(k)$ is computed using equation 4.3.11 and compared to the true channel, $H(k)$. This experiment is repeated for SNR values of 10 dB, 15 dB, 20 dB and 25 dB 200 times and the average is taken; each time the channel is computed using all the virtual carriers and i_{enough} virtual carriers. For this simulation all the pilot symbols, positioned as in the WiMAX specification are used to estimate the channel. In a real life situation some sort of interpolation is then done using the estimated channel at the pilot sub-carriers to compute the channel estimate at the data sub-carriers; however this is not covered in this scope of this thesis. The channel amplitude, $|H(k)|$ is then plotted against the frequency, k for different SNR values as shown below.

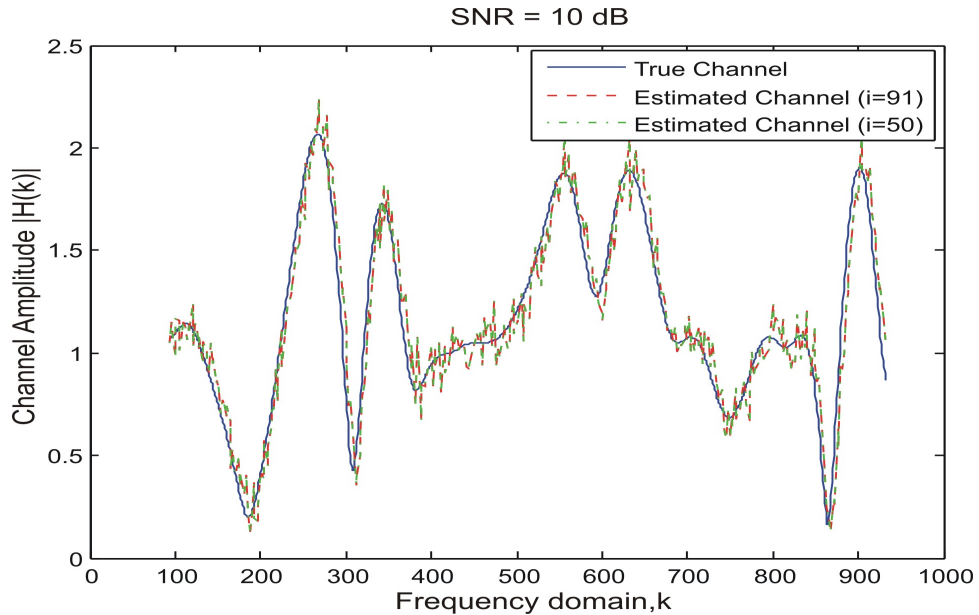


Figure 5.5. Channel Estimate SNR = 10 dB.

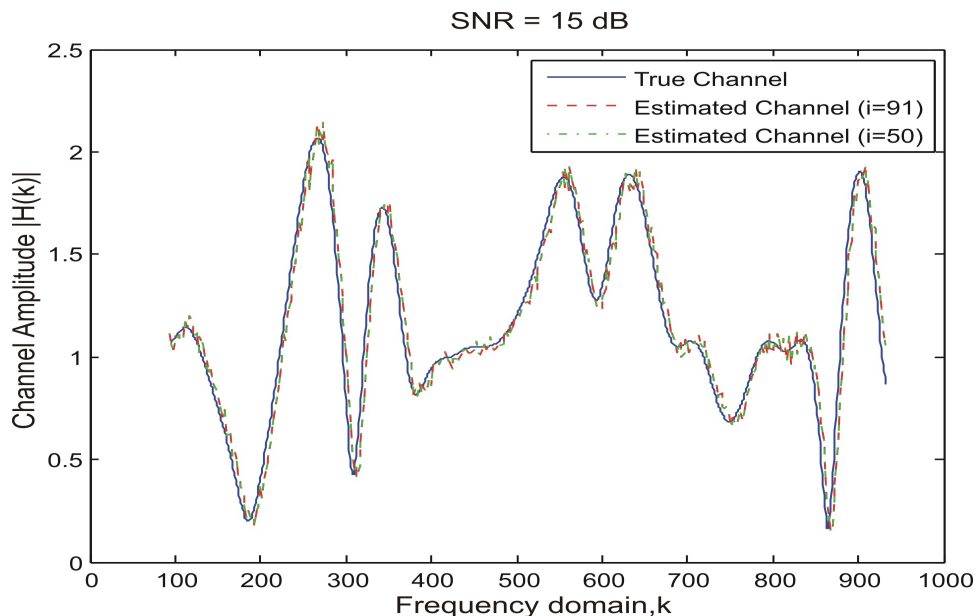


Figure 5.6. Channel Estimate SNR = 15 dB.

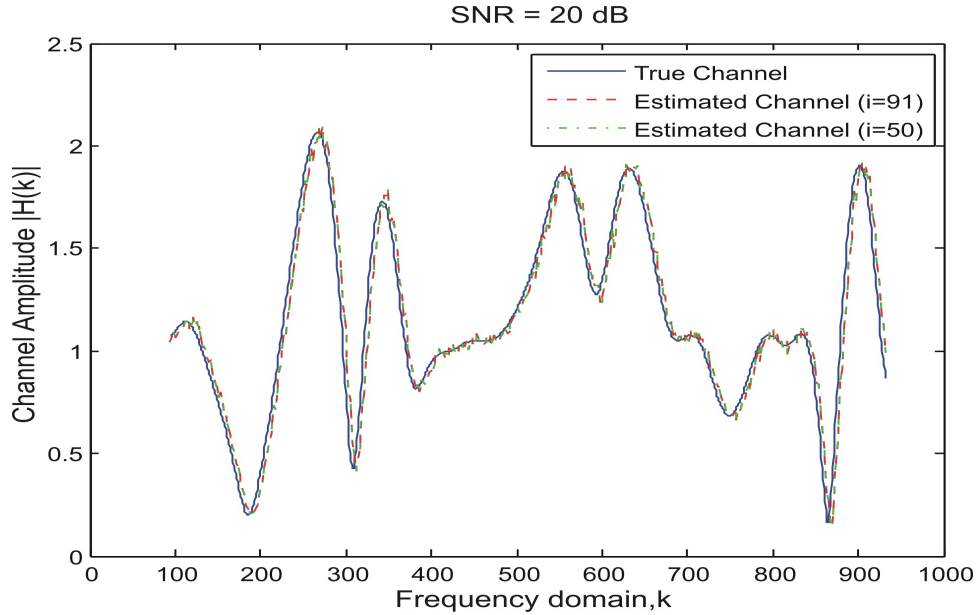


Figure 5.7. Channel Estimate SNR = 20 dB.

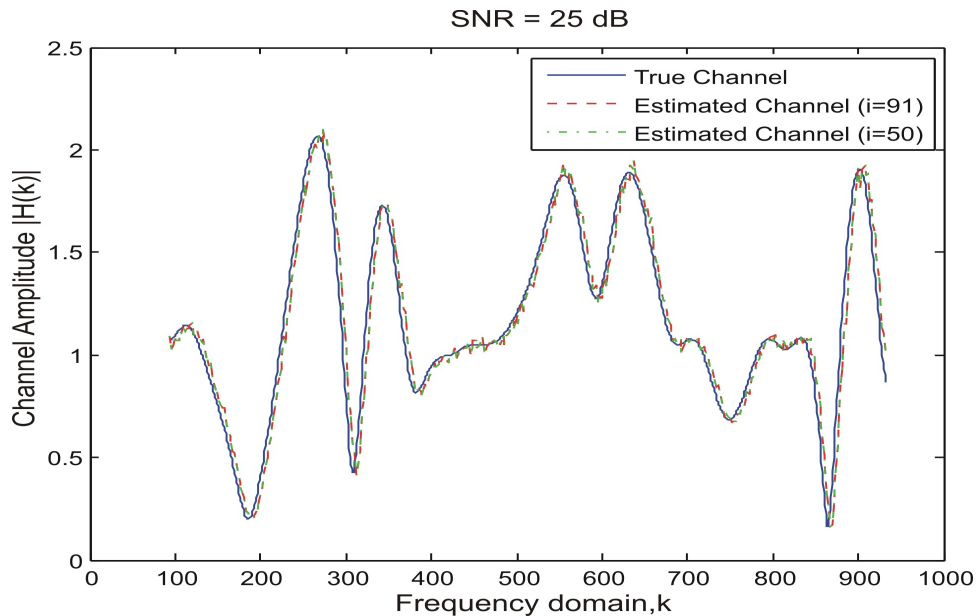


Figure 5.8. Channel Estimate SNR = 25 dB.

For SNR = 10 dB, although the MSE is visibly less when 91 virtual carriers are used for phi estimation compared to when 50 virtual carriers are used; the channel estimates are almost identical. It could then be said from the point of view of channel estimation that 50 virtual carriers are enough for estimation. However, the channel estimate is noisiest compared to the cases of 15 dB, 20 dB and 25 dB.

For SNR = 15 dB and above, the channel estimates are identical. This can be expected since the channel estimate depends on the accuracy of phi estimate, and phi estimate is not affected by the SNR level greater than 15 dB in both the case of using 91 and 50 virtual carriers for estimation.

Chapter 6

CONCLUSIONS

This thesis project gave us a good knowledge of OFDM systems, and a good experience on how to carry out efficient research.

We have presented ML estimation of OFDM carrier frequency offset as well as channel estimation implementation. Unfortunately due to inadequate time available for this thesis work, we could not implement another/other OFDM carrier frequency estimator(s) for the purpose of comparing our findings.

We found that the optimality of ML estimator is not compromised for SNR values over 10 dB, hence the ML estimator works well in a relatively noisy environment.

The ML estimation method, uses the virtual carriers for frequency offset estimation. From this point of view all the virtual carriers not needed for estimation could be used for carrying information. Because our investigations showed that it is enough to use 50 virtual carriers for frequency offset estimation, this could be a motivation to reduce the length of the last guard sub-carriers of OFDM symbols specified in 802.16e. However, further investigation would be needed to ensure that ISI is not a consequence.

Because we are able to understand the structure of the cost function described in equation 4.3.13 in terms of the periodicity of the local minima, we can estimate frequency offset errors which are larger than 2% of the sub-carrier spacing without significant increase in computational cost (as long as the search is carried out in a range where there is a single minimum).

The channel estimation is good for SNR values greater than 10 dB; by using a good interpolation scheme, the true channel can be constructed from the estimates to a high degree of accuracy.

6.1 Future Work

In the future it would be interesting to investigate the time interval necessary between each ϕ estimation, i.e., how many OFDM symbols an estimated phi would be valid for in time-varying channels?. The *MATLAB®* codes used in this thesis would be available at the department for future researchers who are interested in further studies of OFDM.

The focus of this thesis is OFDM carrier frequency estimation; therefore no study was done on different modulation methods, e.g., QPSK, 16-QAM, 64-QAM as well as channel coding. In the future, more work needs to be done on channel coding (FEC) and signal modulation methods as they are used in most practical systems to improve the system performance.

BIBLIOGRAPHY

- [1] Biao Chen, “Maximum Likelihood Estimation of OFDM Carrier Frequency Offset”, IEEE Trans.Signal processing letters, volume 9, no.4, april 2002.
- [2] M Shakeel Baig, “Signal Processing Requirements for WiMAX (802.16e) Base Station”, master thesis, Signal processing group, Department of signal and systems, Chalmers University of Technology, Gothenburg, Sweden, 2005.
- [3] Carin Omurcali, “Channel estimation and its effect on the performance in an OFDM system”, Master’s Degree Project, KTH Signals Sensors and Systems, Stockholm, Sweden, May 2004.
- [4] Mobile WiMAX - Part 1: “A Technical Overview and Performance Evaluation manual” Prepared on Behalf of the WIMAX Forum, 2006.
- [5] P. Moose, “A technique for orthogonal frequency division multiplexing frequency offset correction”, IEEE Trans. Commun., vol. 42, pp. 2000-2914, Oct. 1994.
- [6] Orthogonal Frequency Division Multiplex Synchronization Techniques for Frequency-Selective Fading Channels by Thomas Keller, Lorenzo Piazzo, Paolo Mandarini, and Lajos Hanzo, Senior Member, IEEE. 6, JUNE 2001.
- [7] Richard Van Nee, Ramjee Prasad. OFDM for wireless multimedia communications, Artech house publisher, 2000.
- [8] 3rd Generation Partnership Project; Technical Specification Group Radio Access Networks;Deployment aspects (Release 4) - 3GPP TR 25.943 V4.2.0 (2002-06).
- [9] Space-time codes for high data rate wireless communication:performance criterion and code construction. Tarokh, V.; Seshadri, N.; Calderbank, A.R. Information Theory, IEEE Transactions on Vol. 44, Issue 2, Mar 1998 Page(s):744 - 765.
- [10] Dušan Matiae, “OFDM as a possible modulation technique for multimedia applications in the range of mm waves”, 10/30/98/TUD-TVS.

- [11] Jan-Jaap van de Beek, Magnus Sandell, Per Ola Borjesson, "ML Estimation of Timing and Frequency Offset in Multicarrier Systems", Master Thesis at Div. of Signal Processing, Lule University of Technology, 1999.
- [12] A Mixed OFDM Downlink and Single Carrier Uplink for the 2-11 GHz Licensed Bands - IEEE 802.16 Broadband Wireless Access Working Group.
<http://ieee802.org/16>
- [13] The Cyclic Prefix of OFDM/DMT An Analysis. 2002 International Zurich Seminar on Broadband Communications, Feb 9-21, ETH Zurich. Werner Henkel, Georg Tauböck, Per Ödling, Per Ola Bröjesson, Niklas Petersson, Albin Johansson.
- [14] Lili Zhang, "A study of IEEE 802.16a OFDM-PHY Baseband", Master thesis performed in Electronics Systems, Linköping, 2005.
- [15] S. Coleri, M. Ergen, A. Puri and A Bahai, "A study of channel estimation in OFDM systems", IEEE vehicular technology conference, Vancouver, Canada, September, 2002.
- [16] L.M. Correia, ed., Wireless flexible personalized communications - COST 259: European cooperation in mobile radio research, John Wiley Sons 2001.
- [17] L. Alhin and J. Zander, "Principles of Wireless Communications", Studentlitteratur, Lund 1998.
- [18] John Fox, "Maximum-Likelihood Estimation: Basic Ideas", York Summer Programme in Data Analysis, McMaster University, Ontario, May 2005.
- [19] Draft IEEE Standard for Local and metropolitan area networks "Part 16: Air Interface for Fixed and Mobile Broadband Wireless Access Systems, Amendment for Physical and Medium Access Control Layers for Combined Fixed and Mobile Operation in Licensed Bands, IEEE P802.16e/D6", February 2005.
- [20] S.B Weinstein and P.M. Ebert, " Data Transmission by Frequency-Division Multiplexing Using the Discrete Fourier Transform ", IEEE Trans. Commun vol.19, no.5, 1971.
- [21] C.W. Baum, K.F Conner, "A multicarrier transmission scheme for wireless local communications", IEEE Journal on Selected Areas in Communications, vol. 14, no.3, April 1996.